

# Graphical Design and Analysis of Thermally Coupled Sidestream Columns Using Column Profile Maps and Temperature Collocation

**Daniel A. Beneke**

Dept. of Chemical and Metallurgical Engineering, University of the Witwatersrand, Johannesburg 2050, South Africa  
Laboratory for Product and Process Design, Dept. of Chemical and Bio Engineering, University of Illinois at Chicago, Chicago, IL 60607

**Andreas A. Linninger**

Laboratory for Product and Process Design, Dept. of Chemical and Bio Engineering, University of Illinois at Chicago, Chicago, IL 60607

DOI 10.1002/aic.12453

Published online November 29, 2010 in Wiley Online Library (wileyonlinelibrary.com).

*A systematical procedure is presented to design thermally coupled sidestream units like side rectifiers and side strippers are presented in this article. The method combines the column profile map technique to assess topological characteristics of the specific configuration with temperature collocation to rigorously ensure a realizable column design, without making assumptions with regard to the phase equilibrium or product specifications. The proposed methodology offers a unique graphical insight into the challenging problem of thermally coupled column synthesis. Techniques are presented for highlighting superior designs or eliminating inferior ones, based on vapor flow rate, number of stages, and thermodynamic efficiency. Design parameters such as the feed and side-draw trays that may require insight or experience are products of the procedure. Design solutions obtained using this methodology can be used to initialize the state of the art process flow sheeting tool, AspenPlus<sup>TM</sup>, which typically leads to fast convergence to the desired product purities without further adjustments. © 2010 American Institute of Chemical Engineers AICHE J, 57: 2406–2420, 2011*

*Keywords: side rectifiers/strippers, column profile maps, temperature collocation*

## Introduction

Distillation is the most widely used method in modern chemical industries to separate liquid mixtures into pure components. Despite its wide use and functionality, it is a very energy intensive method of separation, accounting for about 40% of the total energy used in the chemical and petroleum refining industries.<sup>1</sup> With the price of energy and

environmental concerns expected to increase even further, researchers and process engineers have set out to find new and creative ways to operate and design separation units. To this end, the notion of coupling individual columns through transferring heat between them has received considerable attention, with reports that up to 50% average savings on the energy demand may be achieved, when compared with the traditional approach, where simple columns are used in series to achieve the desired product purities.<sup>2–6</sup> These savings arise partly due to the fact that the number of reboilers and condensers are reduced, but it should be noted that these savings are dependant on numerous factors including the

Correspondence concerning this article should be addressed to A. A. Linninger at linninge@uic.edu.

compositions and volatilities of the feed stream.<sup>3</sup> Furthermore, because thermally coupled arrangements reduce the number of reboilers and/or condensers required to affect the separation, significant capital savings can also be achieved.

The simplest method of thermal coupling is a large main column that preseparates the light and heavy components in the feed, linked to a side unit which removes one or more intermediate components. These units, called side rectifiers or strippers or more generally thermally coupled sidestream units, have found considerable use in practice. The side stripping column has been extensively used in petroleum refineries,<sup>7</sup> whereas the side rectifier columns have found application in air separation<sup>8</sup> as well as replacing entrainer regeneration columns in extractive distillation operations.<sup>9</sup> Other, more complex arrangements such as the fully thermally coupled Petlyuk or Kaibel column arrangements have also been proposed, with even greater potential for energy and capital investments. Although thermally coupled structures promise significant cost reductions, their widespread implementation has been hampered somewhat by control and operational problems. The energy integration increases the control loop coupling in the system, so that the operating strategy for the columns is no longer apparent. This could lead to irregular startup and shutdown procedures and may therefore offset any potential savings due to noncontinuous production.<sup>10</sup> However, numerous advances have been made in the operability of coupled columns in recent years,<sup>2,11–15</sup> so much so that large companies like BASF (and others) now have fully functioning Petlyuk and Kaibel columns.<sup>16</sup>

Numerous techniques have been proposed to design thermally coupled side rectifiers and strippers. Several of these methods deploy the Underwood equations,<sup>17–19</sup> but this method is reliable only for nearly ideal and zeotropic systems and also assumes sharp product specifications. The vapor rate and the minimum reflux ratio, both of which are imperative for the column design and cost, will therefore be idealized using the Underwood methods. Another, more recent approach using the shortest stripping line<sup>20</sup> shows a robust energy targeting strategy that provides a continuously differentiable description of column sequences. This approach can account for any phase equilibrium behavior (including azeotropes) and has the ability to find column sequences that contain nonpinched, minimum energy columns within a sequence as well as accounting for heat integration and capital/operational cost trade-offs, using numerical optimization techniques.<sup>21</sup> Rigorous models using tray-by-tray computations which account for nonidealities have also been suggested,<sup>22</sup> but global optimization methods of synthesis problems involving both structural and parametric degrees of freedom is still a challenge for existing math programming algorithms. Furthermore, black box solutions also permit limited insight the designer can derive from the final solution.

Recently, a column profile map technique has been proposed and was shown to be an efficient tool to synthesize distillation columns, including simple and thermally coupled columns.<sup>23–25</sup> The graphical and general nature of this technique mean that the designer is able to achieve considerable insight and flexibility in the design. However, the graphical aspect of this approach has a drawback that it involves trial-and-error for determining parameters to con-

struct and validate composition profiles repeatedly until a suitable design is found.

A temperature collocation approach proposed by Zhang and Linninger transformed the governing equations in the work of Tapp et al. thermodynamically to rigorously synthesize simple columns.<sup>26</sup> More recently, an expansion of temperature collocation has been shown to entire networks of simple and complex column configurations.<sup>27</sup> The advantages of combining the two design approaches are (1) nonideal mixtures may be easily modeled, (2) multicomponent (>4) problems can be designed semiautomatically, (3) any network configuration may be designed and tested for feasibility, and (4) design variables such as the feed tray, side-draw tray and total number of stages can be determined rationally without much computational effort. Furthermore, they showed that the column specifications obtained from this methodology for entire separation networks can be validated with AspenPlus.

This article aims to combine the advantages of the column profile map and temperature collocation techniques, for the rational design of thermally coupled side stripper and rectifier columns. This article does not attempt to find globally optimal solutions to the problem of thermally coupled sidestream column, but instead presents a systematical and rigorous design strategy that offers design engineers clear insight into the behavior of these configurations. This article is structured in the following manner: A “Methodology” section discusses the design methodology and general properties of the column profile map and temperature collocation techniques. The following section highlights the procedure for side stripper/rectifier design including its structural properties, a degree of freedom analysis, mass balance properties, feasibility criteria, and informed choices of design variables. The “Design Trade-Offs” section presents the spectrum of feasible designs for a methanol/ethanol/*p*-xylene case study and specifically methods are proposed to direct one to superior designs based on the reboiler duty, the number of stages, and energy efficiency. This article closes with conclusions summarizing significant results from this work and suggesting areas of future work and applicability of the methods.

## Methodology

### Column profile maps

Continuous column profile equations were originally proposed by Van Dongen and Doherty for conventional rectifying and stripping sections.<sup>28</sup> These continuous equations were expanded to the difference point equation for a generalized column section (CS), from which a column profile map may be constructed, by setting parameters such as the reflux ratio and net compositional flows.<sup>23</sup> The general nature of the column profile map method has the advantage that it is not specific to any configuration, which consequently lends itself to model any structure, irrespective of its complexity. The equations have been developed by defining a CS as a length of column between points of material addition or removal, as shown in Figure 1.

The equation describing the liquid compositional change along the CS may then be derived through a steady-state mass balance over a CS, assuming constant molar overflow followed by a Taylor expansion, which yields:

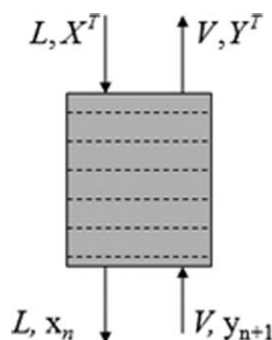


**Figure 1. A generalized column section (CS), with liquid composition  $x$  and  $X^T$ , and vapor compositions  $y$  and  $Y^T$ .**

The superscript T indicates the compositions at the top of the CS, whereas  $n$  indicates a respective tray number.

$$\frac{dx}{dn} = \left( \frac{1}{R_\Delta} + 1 \right) (x - y(x)) + \left( \frac{1}{R_\Delta} \right) (X_\Delta - x) \quad (1)$$

where

$$X_\Delta = \left( \frac{VY^T - LX^T}{V - L} \right)$$

and

$$R_\Delta = \frac{L}{V - L} = L/\Delta$$

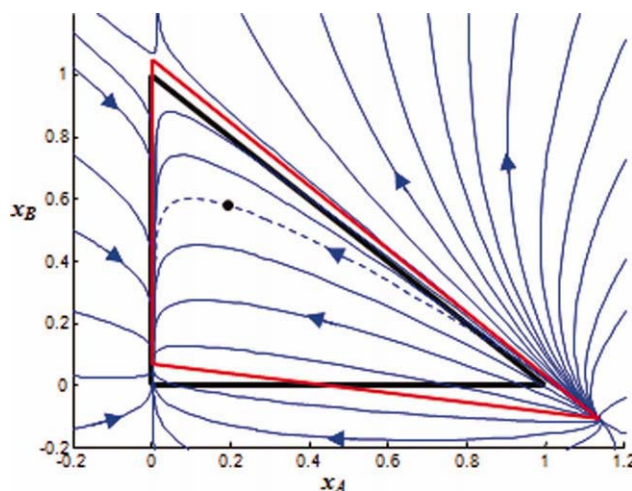
Equation 1 is known as the difference point equation, where  $R_\Delta$  is a generalized reflux ratio in the CS, and  $n$  is the number of stages.  $X_\Delta$  is termed the difference point, which can be thought of as a pseudo composition vector, valid anywhere in the composition space. Like regular compositions, the elements of the difference point sum to unity. Furthermore,  $X_\Delta$  need only be smaller and less than unity in CSs that are terminated by a condenser or reboiler. Negative element entries, corresponding to  $X_\Delta$  located outside the mass balance triangle, merely implies that the respective component is flowing downward in the CS. Accordingly, negative reflux ratios indicate that the section is in stripping mode, i.e., there is a net flow of material down the column ( $L > V$ ) and conversely, positive reflux ratios indicate that a CS is in rectifying mode as there is a net flow of material upward. The vapor composition  $y(x)$  can be related to the liquid composition using an appropriate vapor-liquid equilibrium model. Once the aforementioned parameters have been set a column profile map may be constructed, as shown in Figure 2 for arbitrarily chosen process parameters.

Figure 2 shows that stationary points have been shifted from the pure component vertices (red triangle), which corresponds to a residue curve map ( $R_\Delta = 8$ ). The dashed trajectory in Figure 2 indicates a principal profile as the profile runs through the difference point, which corresponds to a CS producing an actual product cut of composition  $X_\Delta$ . All other profiles are termed secondary profiles, which represents all possible trajectories of complex CSs which obey the same difference point, but originate from different compositions.

Notice that it is mathematically possible to track concentration profiles in regions outside the mass balance triangle.

Even though these profiles are not physically realizable, the expansion of the scope of the topological space provides new insights into the feasibility of separation tasks inaccessible to the traditional view confined within the mass balance triangle. It has been shown that the analysis of negative compositions may add insight to column synthesis, but this is beyond the scope of this article and the reader is referred to Tapp et al.<sup>23</sup> and Holland et al.<sup>29</sup> for a more in depth analysis of the significance and topological effects of parameters, especially in negative composition space. It should be clearly noted, however, that the direction of composition profiles can be altered by a combination of reflux and  $X_\Delta$ , and they can even be attracted to points located outside the real composition space.

To gain a basic understanding into the relation of parameters and general design procedure for the column profile map method, a simple case of a single-feed-two-product column is discussed. In this instance, there are two CSs (rectifying and stripping) and consequently two sets of difference point equation parameters that need to be specified. As a product is being drawn off from both sections via a reboiler/condenser,  $X_\Delta$  corresponds to the product specifications in both sections. As with conventional design methods, an internal column variable also has to be specified, either a reflux or reboil ratio. The generalized reflux ratio,  $R_\Delta$ , is in this case equal to the traditional reflux ratio ( $r = L/D$ ) in the rectifying section. By an energy balance over the entire column, the generalized reflux for the stripping section, which is analogous to the traditional reboil ratio, may also be determined. Once all difference points have been specified and/or calculated, the difference point equation for each CS may be integrated with the product compositions as the starting point. The design given by the purity



**Figure 2. A column profile map with a generalized reflux of  $R_\Delta = 9$  and a difference point of  $X_\Delta = [0.2, 0.6]$  (black dot).**

The dashed blue lines represent principal profiles emanating from the difference point, which corresponds to a CS with a product cut. Secondary column profiles, drawn in solid blue lines, represent CSs with the same difference point as the principal profile but with different entering liquid and vapor compositions. All profiles may be extended beyond the boundaries of the mass balance triangle (in black) for gaining a better understanding of both the topology and pinch points. Each profile approaches the stationary points indicated by the red triangle. [Color figure can be viewed in the online issue, which is available at [wileyonlinelibrary.com](http://wileyonlinelibrary.com).]

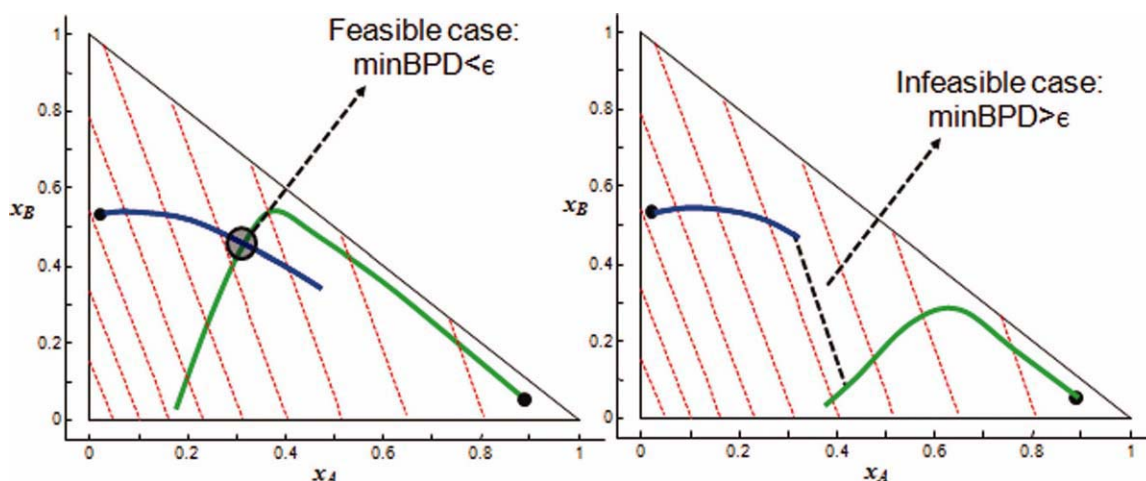


**Figure 3. Distinguishing feasible and infeasible designs using the bubble point distance function.**

Red lines indicate isotherms, whereas green and blue lines are compositional profiles for the rectifying and stripping sections in a simple column, respectively. [Color figure can be viewed in the online issue, which is available at [wileyonlinelibrary.com](http://wileyonlinelibrary.com).]

specifications and reflux ratios is feasible if the concentration profiles of the rectifying and stripping CSs intersect.

### Temperature collocation

The temperature collocation approach, originally proposed by Zhang and Linninger for conventional rectifying and stripping sections is based on a thermodynamic transformation whereby the independent integration variable in the difference point equation is changed from the stage number ( $n$ ) to the tray bubble point temperature ( $T$ ). This transformation has the advantage that designs may be rigorously and quickly assessed in an algorithm using a bubble point distance (BPD) function, which eliminates the dimension of top and bottom trays to a single coordinate, the bubble point temperature. The variable transformation yields a composition profile equation as a function of tray bubble point temperature, given in vector form in Eq. 2:

$$\frac{dx}{dT} = \frac{-\left[\left(1 + \frac{1}{R_{\Delta}}\right)(x - y) + \left(\frac{1}{R_{\Delta}}\right)(X_{\Delta} - x)\right] \frac{dK}{dT} x}{\left[\left(1 + \frac{1}{R_{\Delta}}\right)(x - y) + \left(\frac{1}{R_{\Delta}}\right)(X_{\Delta} - x)\right] K} \quad (2)$$

where  $K$  is the vector of equilibrium constants relating vapor and liquid compositions with each other. The individual components are defined by  $K_i = \frac{\gamma_i(x,T)P_{i,SAT}(T)}{P}$ . Nonidealities can be incorporated into this equation by modeling the liquid activity coefficient with an appropriate phase equilibrium model. Numerical integration can be performed from a known bubble point temperature (i.e., at a product composition) toward the profile termination point, calculated by solving Eq. 2 at steady state conditions.

In all column configurations, simple or complex, a design is feasible if and only if the liquid composition profiles of all adjacent CSs in a configuration intersect one another. In other words, all products are connected by one continuous profile. In terms of the temperature collocation methodology, this implies that the Euclidian distance or bubble point distance (BPD), between liquid composition profiles of adjacent column sec-

tions on a single temperature isotherm is smaller than a certain predefined small tolerance,  $\epsilon$ . This method is conveniently visualized in Figure 3, which shows how the BPD may be used to distinguish between feasible and infeasible designs.

Each trajectory in Figure 3 is essentially divided into a set of predefined finite elements, where each element is fitted with a polynomial containing a predetermined number of roots. This orthogonal collocation on finite elements (OCFE) method thus transforms the problem to a system of nonlinear algebraic equations.<sup>30</sup>

### Design Aspects

This section introduces procedures and properties of side stripper/rectifier design that aids in the understanding of the design of these configurations. Specific focus is given to structural properties and mass balances as well as a suitable choice of design variables which allows the designer to gauge the interaction between all CSs. Ultimately, the graphical design and analysis allows one to gain insight into feasibility conditions and criteria for realizable designs from which a general design algorithm may be devised.

### Structural aspects

Using the definition of a CS, any separation process may be represented by a network of CSs as shown in Figures 4a, b for a side stripper and rectifier, respectively. Interestingly, from a structural point of view, even though these thermally coupled arrangements differ considerably from a conventional sequence of simple columns, the number of CSs in both configurations is equivalent to separate a multicomponent mixture into pure components. In fact, the number of CSs required to separate a  $nc$ -component mixture into pure components, is equal in the thermally coupled sidestream arrangement to any other sequence of conventional simple columns and is always  $2(nc-1)$ .<sup>31,32</sup> However, fully thermally coupled columns such as the Petlyuk column do not follow this trend, and generally require  $nc(nc-1)$  CSs.<sup>33</sup> The CSs in both



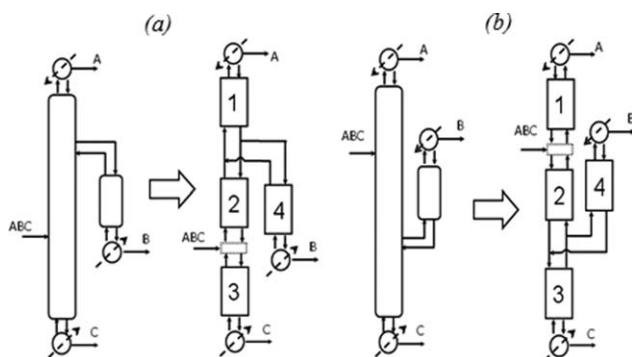


**Figure 4. Basic thermally coupled sidestream columns with the associated column section breakdown for (a) a side stripper and (b) a side rectifier, showing the vapor and liquid distribution at the side draw stage.**

configurations are labeled CS<sub>1</sub> through CS<sub>4</sub> as referred to in Figures 4a, b and all subsequent discussions.

Figures 4a, b also indicate the manner in which the material flows in the thermally coupled CSs are linked to each other. For instance, in the side stripper configuration in Figure 4a, the liquid flowing from CS<sub>1</sub> is divided between CS<sub>2</sub> and CS<sub>4</sub>. The vapor flow in CS<sub>1</sub> is merely a mixture of the vapor flows of CS<sub>2</sub> and CS<sub>4</sub>. The side rectifier operates in an analogous manner; the vapor stream in CS<sub>3</sub> is split between the two adjacent CSs and the liquid stream is a mixture. Furthermore, notice that the relative position of the feed and side-draw stage is reversed in the respective configurations.

### Degree of freedom analysis

For both configurations depicted in Figure 4, the external degrees of freedom for an  $nc$ -component system with  $P$  product flows, may be summarized as follows, for a specified feed: Total unknowns:  $P(1 + nc)$  ( $P$  product flows + compositions in each product)

Mass balance equations:  $-nc$  (number of components)

Summation equations:  $-P$  ( $\sum x_i = 1$  in each product stream)

Total degrees of freedom:  $nc(P - 1)$ .

In a traditional three component thermally coupled side-stream configuration as shown in Figure 4, there are consequently six free variables to be set by the designer. Effectively, this means that setting the compositions in all product streams fixes the product flow rates. Besides the  $nc(P - 1)$  external degrees of freedom, traditional thermally coupled sidestream arrangements also requires two internal flow variables to be specified, i.e., the reflux ratio in two CSs. Globally, a sequence of uncoupled columns that performs the same separation has an equivalent amount of degrees of freedom (internal and external). However, the major difference in the two designs is that the two internal degrees of freedom have a strong dependence on one another, whereas a sequence of simple columns is decoupled. Simply put, the reflux ratios in two simple columns may be chosen independently. Different selections of the internal degrees of freedom do however impact the capital investment as well as the total energy demand and efficiency of the process and therefore optimal choices have to be identified systematically. This point will be addressed in the subsequent discussion.

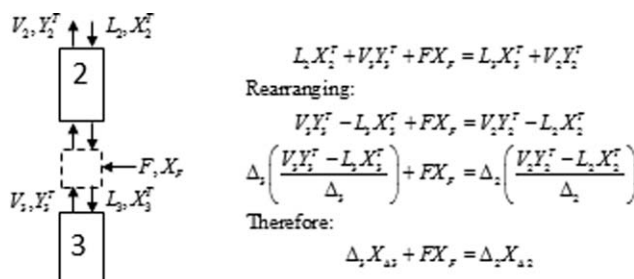


**Figure 5. Mass balance over feed stage.**

### Mass balances aspects

Before designing the entire column configuration, it is important to understand the mass balance constraints on the unit. Figure 5 shows a material balance over the column sections above and below the feed tray for the side stripper configuration shown in Figure 4a, using the definition of  $X_\Delta$  in the difference point equation. Similar mass balance derivations and properties have been demonstrated for the Petlyuk column by Holland et al.<sup>25</sup>

Figure 5 yields a significant result, as it shows that the difference points ( $X_\Delta$ ) above and below the feed tray are linearly related to the feed composition. From a geometric point of view, this relation implies that the feed composition,  $X_{\Delta 2}$  and  $X_{\Delta 3}$  lie on a straight line in composition space. A similar result may be obtained at the thermally coupled side-draw stage for both sidestream configurations, shown in Figure 6 for the side stripper unit.

As CS<sub>1</sub>, CS<sub>3</sub>, and CS<sub>4</sub> in both configurations produce end products and are terminated by a condenser or reboiler, their composition profiles have to be principal profiles because the difference points of these sections are in fact identical to the product compositions in these sections. However, CS<sub>2</sub> does not yield a product cut; its difference point placement is only constrained by mass balance through specifying the other CSs as well as the feed composition. Its column profile will therefore be a secondary profile.

Interestingly, it is entirely possible for Petlyuk arrangements, and other complex configurations, to have difference points that lie outside the mass balance triangle. This property is not even rare and can occur quite naturally in CSs that do not produce end products. This point is discussed more in depth in.<sup>25</sup> However, this case is impossible in side rectifier and stripping arrangements as the difference points of all product producing CSs have to lie inside the mass balance triangle, in consequently the difference point of the internal CS also has to be inside the mass balance triangle. This result is depicted in Figure 7 for both arrangements.

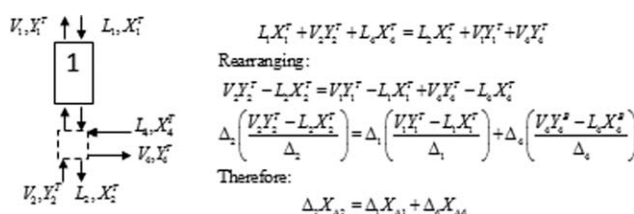


**Figure 6. Mass balance over side-draw stage.**

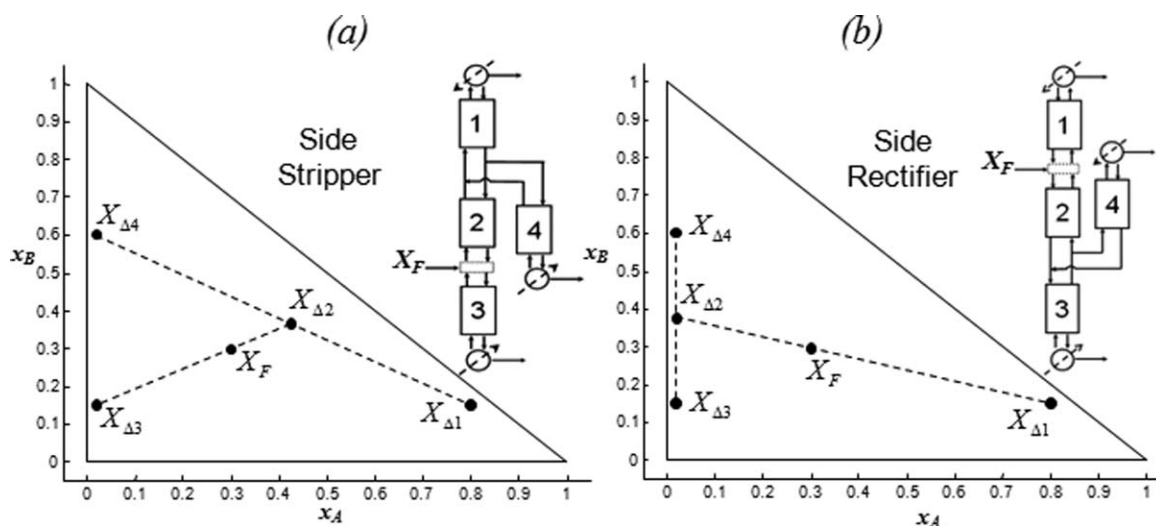


**Figure 7. A geometric interpretation of the difference points for (a) a side stripper configuration and (b) a side rectifier configuration, accompanied by the CS breakdown and numbering of each configuration.**

On both diagrams  $X_{\Delta i}$  is the difference point of the  $i$ th CS.

### Feasibility criteria

Similarly to conventional columns, a thermally coupled column design may be rendered feasible if and only if liquid composition profiles of adjacent CSs intersect. This condition is the same as ensuring that there exists a continuous path of column profiles which connect all products with one another without a gap. Figure 8 shows a feasible side stripper configuration for the ideal benzene/toluene/*p*-xylene system, where all liquid composition profiles intersect. In practice, this criterion means that the bubble point distance is almost zero. The specifications for this separation are summarized in Table 1, where values in bold indicate that they have been specified, whereas other values have been calculated through mass balances.

For this example, the reflux ratios in CS<sub>1</sub> and CS<sub>4</sub> were chosen as the two internal degrees of freedom, although this

choice is completely arbitrary. As mentioned, negative reflux ratios as in CS<sub>3</sub> and CS<sub>4</sub> indicate that a CS is in stripping mode, whereas CS<sub>1</sub> and CS<sub>2</sub> are in rectifying mode. At this point, it is not immediately obvious how the two internal degrees of freedom are related to each other and how one might go about designing an optimal column. These questions will be addressed in the following section.

Notice specifically in Figure 8 that for side stripper configurations, there are three profile intersections in the highlighted area of the side product withdrawal. The liquid composition profiles of CS<sub>1</sub>, CS<sub>2</sub>, and CS<sub>4</sub> all have to share a common point, or in other words, a triple bubble point distance junction. Furthermore, the profiles of CS<sub>2</sub> and CS<sub>3</sub> also have to intersect one another. Because CS<sub>1</sub>, CS<sub>2</sub>, and CS<sub>4</sub> all produce end-products, the composition profiles go through their respective difference points (principal profiles). The internal CS, CS<sub>2</sub>, requires that a so-called secondary profile be constructed, since its starting composition vector is not a difference point.

### Choice of design variables

Using the techniques described in the preceding section allows for an intuitive understanding into the design procedure and attributes of thermally coupled column design. However, it is often the case that the designer needs quick

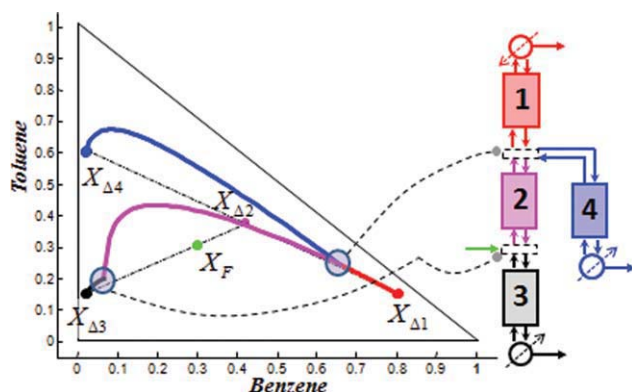


**Figure 8. Feasibility of a side stripper arrangement for the benzene/toluene/*p*-xylene system.**

The bubble point distance between CS<sub>2</sub> and CS<sub>3</sub>, and the triple bubble point distance between CS<sub>1</sub>, CS<sub>2</sub>, and CS<sub>4</sub>, needs to be zero for the side stripper column to be feasible. This criterion is indicated by the highlighted areas. [Color figure can be viewed in the online issue, which is available at [www.interscience.wiley.com](http://www.interscience.wiley.com).]

**Table 1. Stream Table for a Benzene/Toluene/*p*-Xylene System**

Column Section	Difference Point	Reflux	Net flow ( $\Delta$ ) (mol/s)
Feed	[0.300; 0.300; 0.400]	—	1 (pure liquid)
CS <sub>1</sub>	<b>[0.80; 0.150; 0.050]</b>	7	0.359
CS <sub>2</sub>	[0.424; 0.367; 0.209]	1.452	0.692
CS <sub>3</sub>	<b>[0.020; 0.150; 0.830]</b>	−6.524	−0.307
CS <sub>4</sub>	<b>[0.020; 0.600; 0.380]</b>	−4.523	−0.333

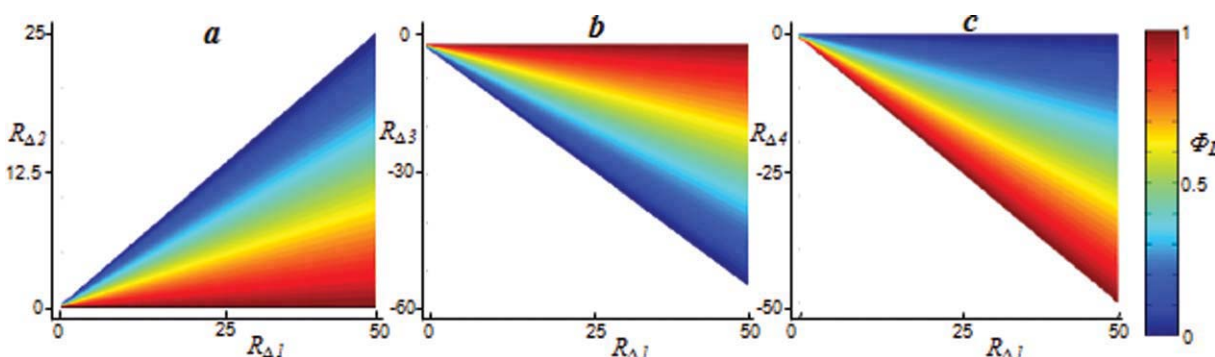


**Figure 9.** Parameter correlation maps for a side stripper showing the influence of  $R_{\Delta 1}$  with varying liquid split ratios ( $\phi_L$ ) on the reflux ratios of (a)  $CS_2$ , (b)  $CS_3$ , and (c)  $CS_4$ .

[Color figure can be viewed in the online issue, which is available at [wileyonlinelibrary.com](http://wileyonlinelibrary.com).]

and reliable answers to the question whether a given set of process specifications are feasible for distillation separation. This task is somewhat more complicated in the case of side rectifiers and strippers, as choosing certain design variables invariably have multiple coupled effects on the entire column. A major design decision in thermally coupled columns is deciding on the internal degrees of freedom. Generally, for the single sidestream arrangement, the reflux ratios of two sections have to be specified. This task is generally not simple one, because reflux ratios can be chosen to lie anywhere between zero and infinity for rectifying sections and zero to negative infinity for stripping sections.

Apart from the fact that reflux ratios are unbounded parameters, it is also difficult to anticipate the interaction between reflux ratios in different CSs. It is more convenient to define a split ratio,  $\phi$ ,<sup>14</sup> which governs the fraction of material sent to the thermally coupled side sections and internal sections. For instance, in the side stripper configuration, we will define a reflux ratio in  $CS_1$  and a liquid split ratio, defined as  $\Phi_L = L_{CS_4}/L_{CS_1}$ , where  $L_{CS_i}$  is the liquid flow rate in the  $i$ th CS and where the subscript  $L$  denotes a liquid-phase split. Analogously for the side rectifier arrangement, the generalized reflux ratio in  $CS_3$  may be specified (effectively the reboil ratio) along with a vapor split ratio  $\Phi_V = V_{CS_4}/V_{CS_3}$ . This specific variable choice narrows the search for a feasible design because  $\phi$  is a bounded dimensionless parameter valid only between zero and one. Even though the defined split ratios narrow the search space somewhat, it is not immediately obvious which combination of split ratios and reflux ratios the designer should choose. The interaction between different choices will be demonstrated next.

**Side Stripper Column Section Interaction.** It is helpful to visually comprehend the effects and interaction that our choices of internal design variables have on other CSs. To this end, parameter correlation maps are a particularly useful tool, which are presented and discussed for both the side stripper and side rectifier. For simplicity, a liquid feed ( $q = 1$ ) with an equimolar composition has been chosen, with pure bottoms, intermediate, and distillate products for both configurations. Although these parameter correlation maps may vary for different feed and product specifications, their qualitative interpretation is similar for all systems. It is important to point out that these regions do not indicate regions of feasibility, but merely show the correlation of CSs for certain combinations of design variables.

Figures 9a–c show the effects on the reflux ratios in a side stripper of the two chosen internal degrees of freedom ( $R_{\Delta 1}$  and  $\phi_L$ ) on  $CS_2$ ,  $CS_3$ , and  $CS_4$  respectively. From Figure 9, it may be inferred that there are for any combination choice of the free design variables, there are always two pairs of equivalent rectifying ( $CS_1$  and  $CS_2$ ) and stripping ( $CS_3$  and  $CS_4$ ) sections. A specific example of the relationship between CSs can be seen, for instance, for a reflux ratio of 25 and a split ratio of 0.5 (the green region on the color bar), which corresponds to generalized reflux ratios of 6.6,  $-15.2$ , and  $-13.8$  in  $CS_2$ ,  $CS_3$ , and  $CS_4$ , respectively.

An important factor to consider is the interaction of reflux ratios in CSs that have utilities attached to them ( $CS_3$  and  $CS_4$ ), as these are major contributors to the operating cost of the column.  $CS_3$  requires its reboiler to operate at a higher temperature than  $CS_4$  as it has to operate at the boiling point of the highest boiling component, whereas  $CS_4$  only operate at the boiling point of the intermediate boiling component. In general, it can be said that it is more expensive to operate a  $CS_3$  reboiler than a  $CS_4$  reboiler when both are operating at equivalent refluxes.

**Side Rectifier Column Section Interaction.** Analogously to the side stripper, parameter correlation maps may be obtained for the side rectifier indicating the relationship of the two chosen design variables ( $R_{\Delta 3}$  and  $\phi_V$ ) on the reflux ratios of  $CS_1$ ,  $CS_2$ , and  $CS_4$  as shown in Figures 10a–c, respectively. Again there are two pairs of equivalent rectifying and stripping sections, but intuitively the role of specific CSs have changed when compared to the side stripper: The internal CS,  $CS_2$ , and  $CS_4$  are in stripping mode, whereas both  $CS_1$  and  $CS_3$  are in rectifying mode. Specifically notice that for a choice of  $R_{\Delta 3} = -25$  and  $\phi_V = 0.5$  (the green region on the color bar), the respective corresponding refluxes in  $CS_1$ ,  $CS_2$ , and  $CS_4$  are 11.2,  $-7.5$ , and 12.5, respectively.

Noticeably, the side rectifier unit only contains one reboiler and consequently all the vaporization takes place in  $CS_3$ . Thus, generally the reflux ratio required in this section is larger than the reflux ratio in the corresponding section ( $CS_3$ ) of the side stripping unit where the reboil duty is divided between two CSs. Although the cost of operating reboilers are, in relative terms, much more expensive than condensers, it is still worthwhile considering what the qualitative effects of our process decisions are on the condensing load. The two condensing units in this configuration are  $CS_1$  and  $CS_4$ . Here,  $CS_1$  is the lowest temperature at which

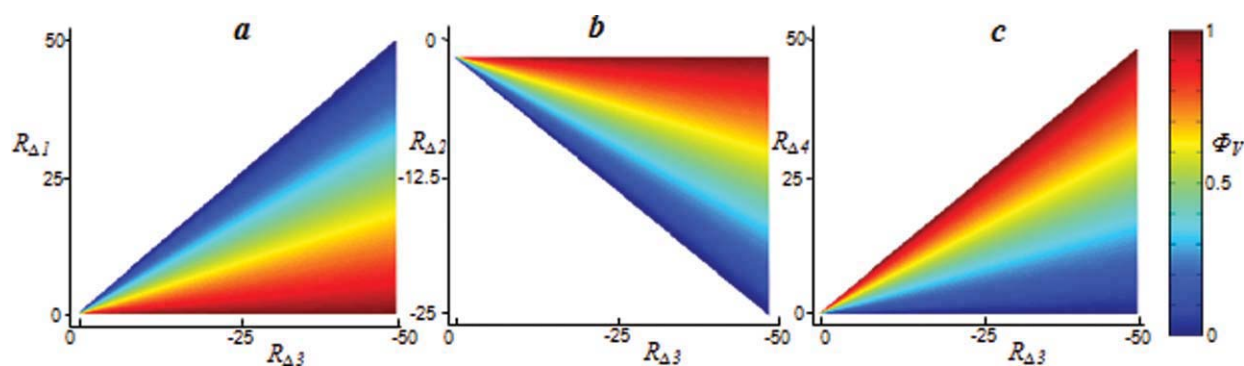


**Figure 10. Parameter correlation maps for a side rectifier showing the influence of  $R_{\Delta 3}$  with varying vapor split ratios ( $\phi_V$ ) on the reflux ratios of (a) CS<sub>1</sub>, (b) CS<sub>2</sub>, and (c) CS<sub>4</sub>.**

[Color figure can be viewed in the online issue, which is available at [wileyonlinelibrary.com](http://wileyonlinelibrary.com).]

condensing takes place and therefore requires a lower duty than an equivalent reflux ratio in CS<sub>4</sub>.

**Additional Design Constraints.** It is apparent from the previous discussion that some of the complexities that arise in thermally coupled sidestream columns are due to the fact that there are multiple reboilers/condensers operating at different temperature levels, as well as multiple and simultaneous effects on all CSs for a certain selection of design variables. Apart from the interaction between CSs, there is however a further constraint to be considered, when deciding on a reflux and/or split ratio, which is the constraint that the external mass balance places on the system. In short, a product producing CS has to have a minimum flow of material flowing into it, which is greater than the amount of product that has to be drawn off from that section. For example, the liquid material that is directed toward the side stripper from CS<sub>1</sub> has to be greater than the amount of intermediate product calculated by the overall mass balance. In general, there are two such constraints for each system. For the side stripper, in terms of our two chosen variables ( $R_{\Delta 1}$  and  $\phi_L$ ), these constraints are given in Eq. 3:

$$\Phi_L \geq \frac{i}{R_{\Delta 1} \dot{D}} \quad \text{and} \quad \Phi_L \leq 1 - \frac{\dot{B} - \dot{F} \times q}{R_{\Delta 1} \dot{D}} \quad (3)$$

For the side rectifier, in terms of our two chosen variables ( $R_{\Delta 3}$  and  $\phi_V$ ), in Eq. 4:

$$\Phi_V \geq \frac{i}{(-R_{\Delta 3} - 1)\dot{B}} \quad \text{and} \quad \Phi_V \leq 1 - \frac{\dot{D} - \dot{F} \times (1 - q)}{(-R_{\Delta 3} - 1)\dot{B}} \quad (4)$$

where  $\dot{D}$ ,  $\dot{B}$ ,  $\dot{I}$ , and  $\dot{F}$  are the flow rates of the distillate, bottoms, side, and feed streams, respectively, and  $q$  is the thermodynamic condition of the feed. Graphically, these constraints can be summarized in  $R_{\Delta} - \phi$  space for both configurations, as shown for the sharp split scenario as described in Figure 11.

Figure 11 indicates that the search space has been considerably reduced for deciding on operation parameters. The side stripper has only one meaningful constraint for this particular system, as the other constraint is above the maximum allowable value for  $\phi_L$ . This is due to the fact that the CS<sub>3</sub> (the distillate CS) always has enough material entering it as the feed has been assumed to be pure liquid and hence all the feed is solely directed to this CS and will never violate the mass balance. However, for different thermodynamic feed compositions there will be multiple constraints on the system, as for the side rectifier arrangement in Figure 11b. As the product

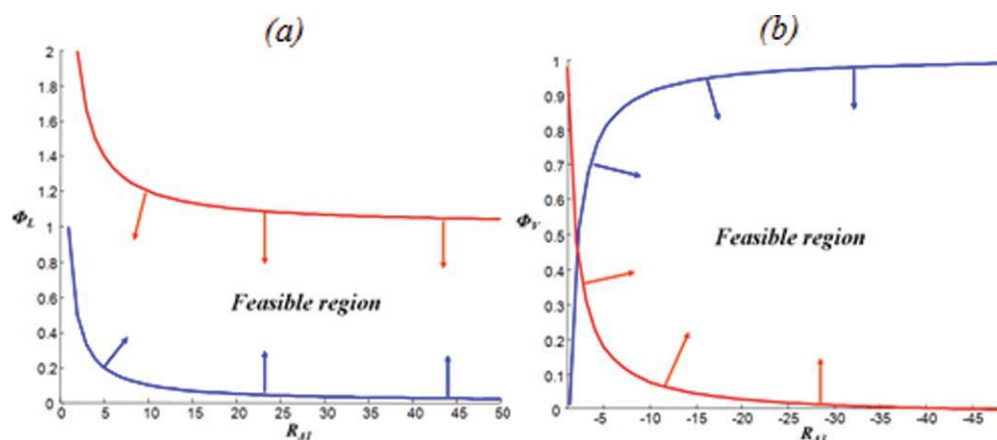


**Figure 11. Feasible operating regions in  $R_{\Delta} - \phi$  space for an equimolar feed and sharp split product specifications from external mass balance constraints for (a) the side stripper and (b) the side rectifier.**

[Color figure can be viewed in the online issue, which is available at [wileyonlinelibrary.com](http://wileyonlinelibrary.com).]



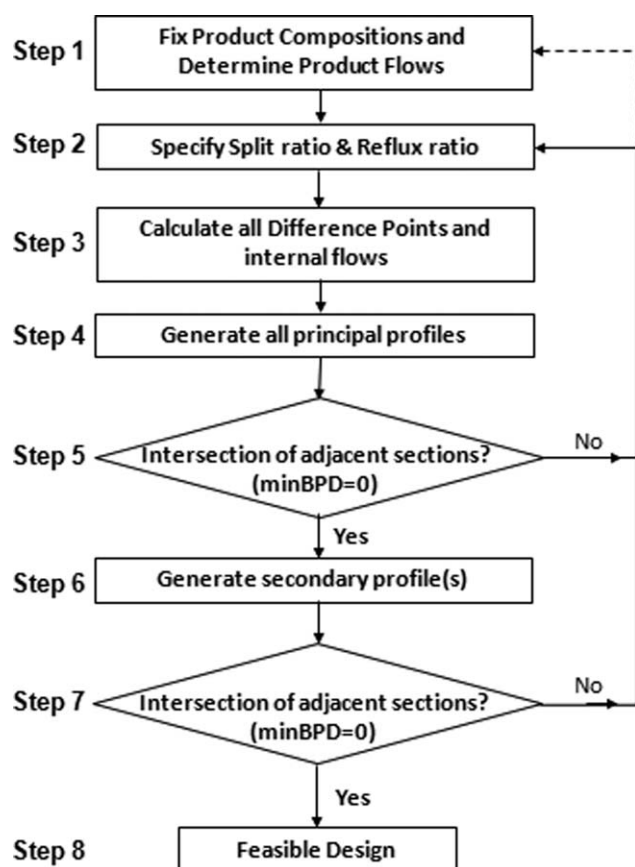


**Figure 12. An information flow diagram for the systematic design of thermally coupled sidestream columns.**

Feasible designs require all bubble points distances to be zero.

and feed specifications determine the product flows, a different specification will result in different feasible regions.

### Automatic design procedure

With a greater understanding about the interaction of process variables and the degrees of freedom available for manipulation by the designer, it is possible to devise a general design algorithm. The set of steps shown in Figure 12 allows one to systematically find feasible solutions quickly and efficiently. Using the temperature collocation approach with the minimum BPD as feasibility criterion allows one to judge a certain structure's feasibility in an algorithmic, computational manner.

The algorithm requires in the first step for the designer to set all product specifications. In step two, the internal degrees of freedom are specified. Once steps one and two have been completed, all difference points and internal flows may be determined in step 3. Step 4 requires one to construct all principal profiles in CSs that produce final products. The subsequent step evaluates whether there is intersection between two adjacent sections, which means the BPD criterion has been satisfied. If this BPD condition is met, the secondary profiles may be generated in Step 6 starting from the intersection point. Step 7 evaluates the second profile intersection, and if the BPD is again within the specified tolerance, a feasible

design has been found. However, if Step 5 or 7 violates the BPD requirement, the procedure requires that either the product specifications or the internal degrees of freedom (or both) have to be modified. With these new specifications, the procedure may be repeated until a feasible design has been found.

Once all feasible design specifications have been identified, we may then proceed to judge which of the feasible designs is optimal with respect to some predefined objective function. A frequently used objective function in distillation design is minimum vapor flow as this usually corresponds to minimum energy usage. However, as discussed in previous sections, it is not trivial in thermally coupled sidestream units because there are several utility inputs at multiple temperature levels which have to be optimally balanced. This point is discussed more in depth in the following example.

### Design Trade-Offs

By setting the product and feed specifications and executing the design algorithm described in the preceding section with a continuous combination of the chosen internal design variables for each system, we are able to obtain a spectrum of feasible design solutions. Once all governing equations have been determined, a computer can, relatively quickly and efficiently, render feasible solutions and assess them with respect to suitable objective functions. In this section, we shall evaluate a side rectifier/stripper design case study for the methanol/ethanol/*p*-xylene system using the nonrandom two liquid (NRTL) activity coefficient model to predict VLE behavior. The NRTL model is used in all cases to demonstrate this method's ability to model any given system and does not need to make idealized assumptions regarding the VLE behavior. The methanol/ethanol/*p*-xylene system, although being zeotropic, displays significant nonideal behavior that cannot be sufficiently modeled with the assumption of ideal phase equilibrium, as seen in the comparative residue curve map in Figure 13.

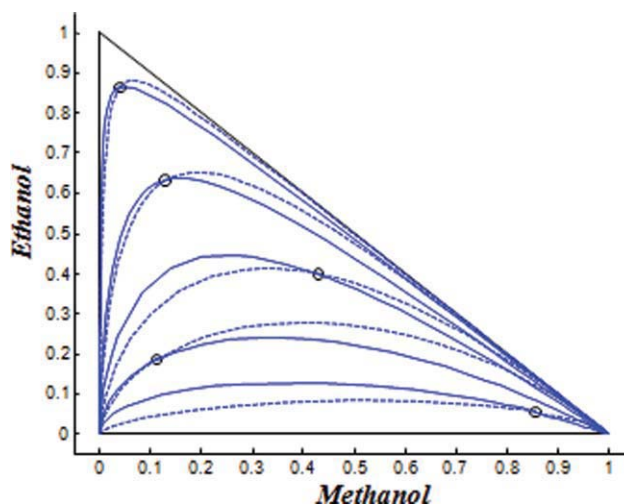


**Figure 13. A residue curve map for the nonideal, zeotropic methanol/ethanol/*p*-xylene system.**

The black circles indicate the points at which integration is initialized using an ideal model (dashed trajectories) and the NRTL model (solid trajectories). [Color figure can be viewed in the online issue, which is available at [wileyonlinelibrary.com](http://wileyonlinelibrary.com).]

**Table 2. Summary of Feed and Product Specifications for the Methanol/Ethanol/*p*-Xylene System with Coefficients for the Antoine Equation Calculated by  $\text{Log}(P_{\text{SAT}}) (\text{mm Hg}) = A - B/(T(^{\circ}\text{C}) + C)$**

Component	Mole Fraction				Antoine Coefficients [A, B, C]
	Feed	Distillate	Side	Bottoms	
Methanol	0.3333	0.9000	0.0800	0.0001	[8.072, 1574.990, 238.870]
Ethanol	0.3333	0.0999	0.9100	0.0499	[8.112, 1592.864, 226.184]
<i>p</i> -Xylene	0.3334	0.0001	0.0100	0.9500	[6.991, 1453.430, 215.307]

Figure 13 shows large deviations from ideal behavior for this particular system, implying that the final design solution is strongly dependant on idealized assumptions regarding the thermodynamic model. The feed and product specifications, along with the Antoine vapor pressure coefficients are summarized Table 2, followed by the NRTL equation used to incorporate nonideal mixtures in Eqs. 5 and 6.

The NRTL equation for methanol ( $i = 1$ ), ethanol ( $i = 2$ ) and *p*-xylene ( $i = 3$ ) for parameters obtained from the Apen-Plus properties database (AspenPlus):

$$\gamma_i = \exp \left[ \frac{\sum_j x_j \tau_{ji} G_{ji}}{\sum_k x_k G_{ki}} + \sum_j \frac{x_j G_{ij}}{\sum_k x_k G_{kj}} \left( \tau_{ij} - \frac{\sum_m x_m \tau_{mj} G_{mj}}{\sum_k x_k G_{kj}} \right) \right] \quad (5)$$

where  $\tau_{ij} = a_{ij} + b_{ij}/T(^{\circ}\text{K})$ ,  $G_{ij} = \exp(-c_{ij}\tau_{ij})$ , and :

$$a = \begin{bmatrix} 0 & 4.7119 & 0.6776 \\ -2.3127 & 0 & 4.0754 \\ -3.2587 & -5.6391 & 0 \end{bmatrix}, \quad (6)$$

$$b = \begin{bmatrix} 0 & -1162.29 & 295.535 \\ 483.8436 & 0 & -1202.43 \\ 1677.6212 & 504.2010 & 0 \end{bmatrix},$$

$$c = \begin{bmatrix} 0 & 0.3 & 0.47 \\ 0.3 & 0 & 0.3 \\ 0.47 & 0.3 & 0 \end{bmatrix}$$

Using an inverse design methodology, the product specification will be the primary concern when searching for feasible solutions. Hence, a solution is acceptable only if the exact product specification is met. The product specifications given here obtain a purity of at least 90% in each product stream. These rough targets have been chosen merely for the purpose of illustrating the method and to obtain a sufficiently large spectrum of feasible designs. Furthermore, notice that the product specifications are nonsharp, to exemplify that the proposed method is not bound by sharp split product restrictions. As mentioned in the “Methodology” section, thermally coupled sidestream columns have two internal degrees of freedom to be specified. It is thus convenient to compare design trade-offs in terms of the split ratio and reflux ratio for each configuration. This is shown in Figure 14, which depicts the spectrum of feasible solutions and the effect on the total reboiler duty (kJ/s) for a feed of 1 mol/s. The overall reboiler duty is equal to the total reboiler duties in each configuration. It should be noted that the regions of feasibility depicted here are strictly system specific, and one may find entirely different regions depending on the phase equilibrium behavior, product, and feed specifications, etc.

The design spectra in both Figures 14a, b were constructed by automatically evaluating 10,000 different combinations of free design variables for each configuration and show that there exists a unique region for each configuration where designs may be realized. Any combination of the two internal values that correspond to the colored region in Figure 14 produces a feasible design. However, all feasible designs are not equivalent which gives an opportunity for the assessment of good designs, or at least eliminating bad

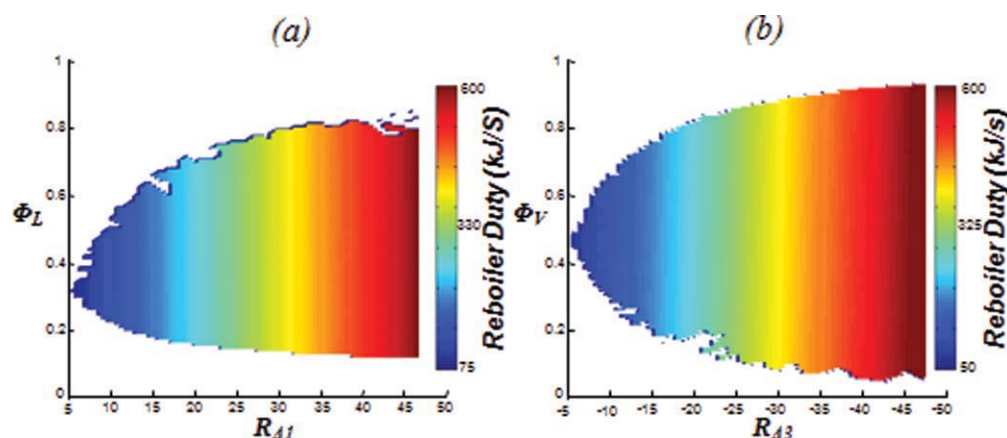


**Figure 14. Spectrum of feasible designs for (a) the side stripper in  $\phi_L - R_{A1}$  space and (b) the side rectifier in  $\phi_V - R_{A3}$  space, showing the effect on the total reboiler duty required in the columns.**

[Color figure can be viewed in the online issue, which is available at [wileyonlinelibrary.com](http://wileyonlinelibrary.com).]

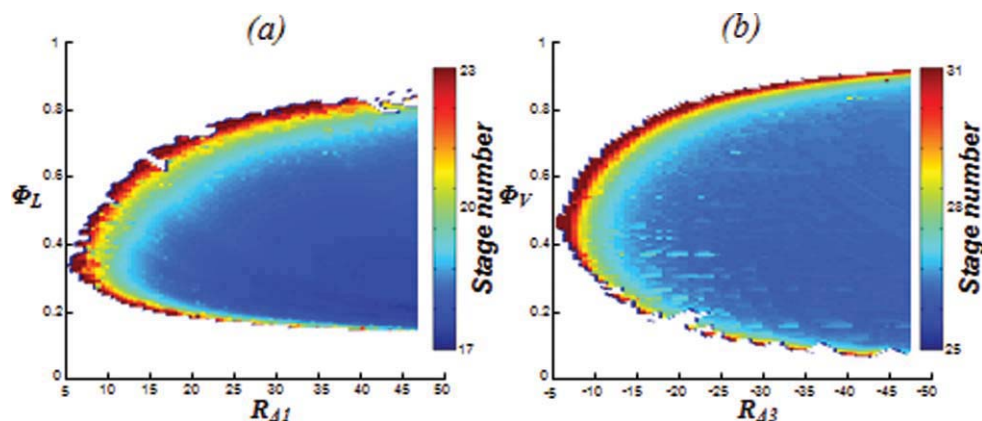


**Figure 15. Spectrum of feasible designs for (a) the side stripper in  $\phi_L - R_{\Delta 1}$  space and (b) the side rectifier in  $\phi_V - R_{\Delta 3}$  space, showing the effect on the total number of stages required in the columns.**

[Color figure can be viewed in the online issue, which is available at [wileyonlinelibrary.com](http://wileyonlinelibrary.com).]

design decisions. Intuitively, Figure 14 shows that the total reboiler duty is minimized when the specified reflux ratio in each configuration is minimized, and vice versa. Furthermore, the reboiler duty of the side stripper is a weak function of the split ratio, because the components in the system have very similar molar latent heat of vaporization. Because there is only one reboiler in the side rectifier, it is entirely independent of the split ratio.

There are several valuable conclusions that may be drawn from Figure 14. First, at the lower ends of the reflux spectrum in this example the side stripper feasible design region is smaller than that of the side rectifier. The spectrum of the side rectifier is much closer to split ratios of zero and one, whereas that of the side stripper is narrower. However, the feasible design region for both these configurations in this case study is infinitely large as feasible designs can still be found at infinite reflux. The feasible regions depicted for both configurations indicate that they both have some degree of operability. The larger feasible space open to the side rectifier permits its operation in a wider range compared with the side stripper unit. The additional flexibility may be of relevance in some processing plants. Second, even though the relative sizes and shapes of feasible design spectra differ considerably, the range of reboiler duties that suffices the product splits in both configurations are relatively similar, but the side rectifier has a slightly lower minimum duty of  $\sim 50$  kJ/s, whereas the side stripper requires around 75 kJ/s. Operating at minimum reflux is however an impractical condition. As the ranges for reboiler duty are relatively similar, we can conservatively state both designs are equivalent with no significant advantage that may be gained in either one in terms of heat requirements. However, it will become apparent in subsequent sections, there are several factors which distinguish these designs.

### Capital cost

The reboiler heat demand in a distillation unit constitutes the majority of the operating cost in a distillation unit. Hence, we may conclude from a first-law point of view that minimum reflux is the optimal operating condition. However, as with conventional columns, operating at minimum reflux

requires an infinite number of stages and hence some compromise between these extremes have to be sought. By combining the temperature collocation with the column profile map approaches, it is possible to obtain an expression that allows for the calculation of number of stages too, as shown in Eq. 7.

$$\frac{dn}{dT} = \frac{\partial n}{\partial x} \frac{\partial x}{\partial T} = \frac{\frac{dK}{dT} x}{\left[ \left( 1 + 1/R_{\Delta} \right) (x - y) + \left( 1/R_{\Delta} \right) (X_{\Delta} - x) \right] K} \quad (7)$$

Using the same approach as above, but applying it to show how the number of stages change in the respective feasible regions results in Figure 15. Our analysis accounts for the amount of stages in the main column as well as the side unit.

It may be seen that, as with distillation design for conventional columns, the designer is faced with a trade-off between two extreme operating choices. Operating at minimum reflux generally corresponds to infinitely many stages, but if one is willing to compromise on first law expenditures, a smaller column may be constructed resulting in reduced capital costs. In both configurations, there is a sharp rise in the number of stages required for a feasible separation as one approaches minimum reflux. The side stripper configuration seems to have a distinct advantage in this instance, as generally for any specific reboiler duty (see Figure 14) a saving of about 6–8 stages can be achieved. At the high end of the reflux spectrum in both configurations, the stage numbers start to level off and no further capital cost saving can be achieved.

### Energy efficiency

A unique property of side rectifier/stripper columns are the multiple temperature levels to which heat is added to the reboiler(s) or rejected in the condenser(s). Although there are a multitude of factors that may influence the final choice on how much heat should be generated at a certain temperature (economics, heat integration with other process, heat availability,



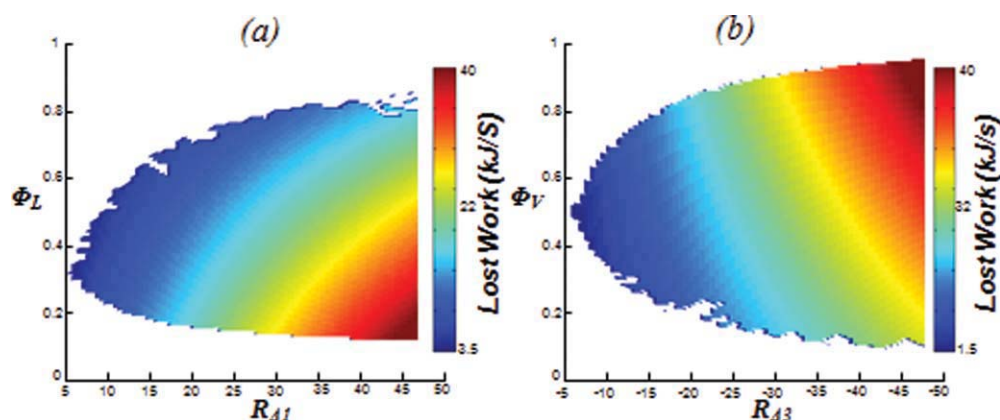


**Figure 16. Spectrum of feasible designs for (a) the side stripper in  $\phi_L - R_{\Delta 1}$  space and (b) the side rectifier in  $\phi_V - R_{\Delta 3}$  space, showing the effect on the lost work produced in the columns.**

[Color figure can be viewed in the online issue, which is available at [wileyonlinelibrary.com](http://wileyonlinelibrary.com).]

etc.), a second-law thermodynamic analysis is a valuable method of judging operating conditions in accordance with the modern drive toward energy efficient processes. Such an analysis will direct one toward the most thermal efficient process by searching for the minimum amount of lost work (LW) generated. The LW calculation is given in Eq. 8 by:

$$LW = T_0 \left( \sum \frac{Q_R}{T_R} - \sum \frac{Q_C}{T_C} + \Delta S_{MIX,F} - \Delta S_{MIX,P} \right) \quad (8)$$

where  $Q_R$  and  $Q_C$  are the heat duties in the reboiler and condenser calculated by the product of the respective vapor flow rates and the composition weighted latent heats of vaporization.  $T_R$  and  $T_C$  are the temperatures at which the corresponding units require or reject heat at and  $\Delta S_{MIX}$  is the entropy of mixing of product (P) and feed (F) streams, given by definition in Eq. 9 as:

$$\Delta S_{MIX} = -R \sum_{i=1}^{nc} x_i \ln(x_i) + S^E \quad (9)$$

where  $S^E$  is the excess entropy for taking nonideal mixtures into account calculated here by the NRTL activity coefficient model, and  $R$  is the universal gas constant. This entropy model allows one to assess process alternatives based on the thermal efficiency, as shown in Figure 16.

The LW calculation provides additional insight into which split ratio to choose to achieve a thermodynamically efficient process. For the side rectifier, the LW is minimized at low-split ratios for a specific reflux, i.e., where less material flow is directed toward the side rectifying unit. The side stripper unit indicates that the minimum LW occurs at higher split ratios, i.e., where more material is directed toward the side stripper. As with the reboiler heat demand however, both units seem to generate similar quantities of LW at the lower end of the spectrum, and from a second-law point of view no structure seem to be advantageous when operating near the lower feasibility bound.

## Finalizing the Design

From the relatively simple calculations shown above it may be inferred that, from an energy usage and efficiency point

of view, both structures are qualitatively similar. However, the side stripper does offer a marked improvement in the number of stages required; hence for this design, we shall choose the side stripper. Guidelines reported in literature<sup>34,35</sup> state that, depending on the system, it is desirable to operate at around 1.05–1.5 times minimum reflux to ensure the amount of stages required do not rise too sharply. By comparing all the analyses for stage number and reboiler duty in the side stripper, we decide on operating at a reflux of 13 as this is the point where the number of stages starts to plateau. Refluxes lower than 13 typically lead to a rapid rise in the number of stages. Finally, the second-law analysis indicates that the most efficient columns are at a high-split ratio, but one should still be aware of the rapid growth in the number of stages. Using these guidelines, conservative design parameters may then be chosen. In this case, a reflux of 13 and a split ratio of 0.45 seems like a good choice, resulting in  $n = 20$  equilibrium stages. It should be noted however that this example is merely an illustration of the applicability of the temperature collocation with column profile map approach to thermally coupled side-stream column design, and the optimal results may vary with a different objective function for design.

A valuable attribute of the methods described in this article is a method to solve the inverse design problem. Product specifications are set and then internal degrees of freedom specified globally until a feasible design range is identified. If the feasible design space is empty, it can be guaranteed that the product specifications are thermodynamically impossible to realize. Process simulation packages such as Aspen-Plus have been shown to be an effective and robust tool for interactive process design. In general however, distillation design in such packages is performed by forward performance simulation which predicts product purities based on a given feed and column design specifications (e.g., total column tray, feed tray, reflux ratio, etc.). Although these packages rigorously solve mass, equilibrium, summation, and enthalpy (MESH) balances, this approach has the drawback that the designer has to have precise initialization knowledge about the design, and it can be a tedious task to search for design specifications that precisely meet the desired product quality. Furthermore, user effort and adjustment is often proportional to the complexity of the system. Because of this



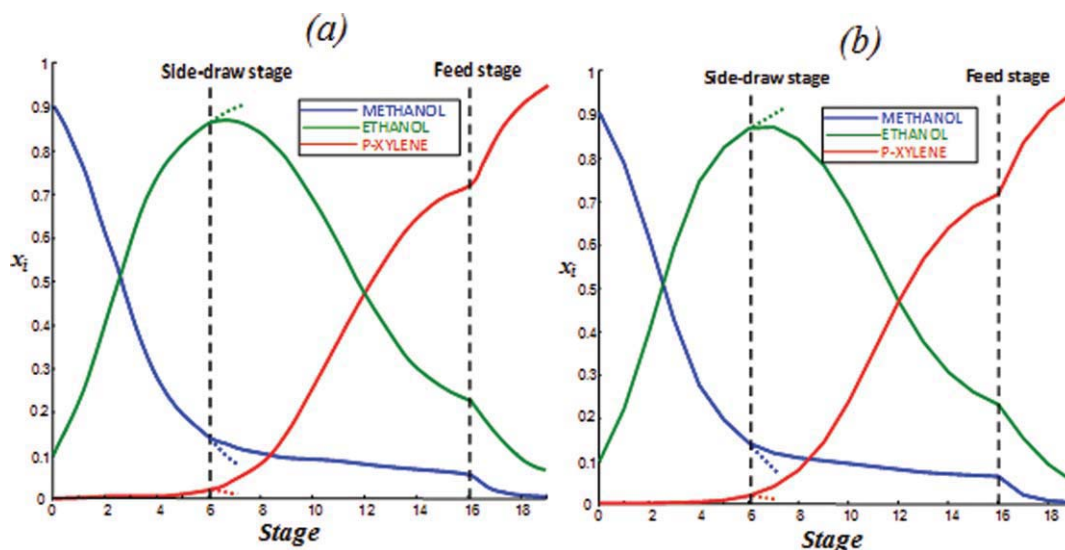


**Figure 17.** Change in liquid composition along the length of the side stripper unit using (a) the temperature collocation method and (b) using AspenPlus with precise initialization from the temperature collocation method.

The main column and side stripper are represented by the solid and dashed lines, respectively. [Color figure can be viewed in the online issue, which is available at [wileyonlinelibrary.com](http://wileyonlinelibrary.com).]

fact, for thermally coupled configurations it is even harder to achieve convergence to the desired product purities. However, using the method advocated in this article, the designer is able to set the product specifications, and from this determine what the structural and operating characteristics of the column are.

Once a general idea of the design has been obtained, the results may be used to initialize a process simulator such as AspenPlus for the chosen design specifications. Even parameters that require a large amount of insight or design experience to obtain, such as the location of the feed tray or side-draw trays, can be easily found by locating the stage number where composition profiles intersect. For this design, the side-draw stage and feed stage were found to be at stages 6 and 16, respectively. For this same scenario, the compositional change in the liquid is then verified with AspenPlus. The resulting profiles depicted in Figure 17 show an excellent agreement with one another.

Small discrepancies in the comparison of compositional change between the proposed method and AspenPlus may be attributed to the assumption of constant molar overflow in the column profile map method. The differences in compositions predicted by our method agrees very well with AspenPlus because the latent heats of all components are very similar and thus the constant molar overflow assumption holds well. At relative high purities, the differences are small but get slightly worse when the mixture is impure, caused by nonideal heat effects of mixing. However, notice that the product specifications have been very closely met. Using the information obtained from the above design procedure as input to an AspenPlus simulation generally leads to convergence within a few seconds. Thus, using the techniques

described in this work, one can save on valuable engineering design time as well as gain a unique graphical insight into the problem and interaction of all operating variables.

#### Extension to higher order systems

The preceding discussions handled the generic case of a single side stripper and rectifier for a ternary system. For higher order systems, i.e., for systems containing more than three components, the design algorithm using the techniques described above can be naturally extended without any modification. However, it should be noted that in higher dimensions, exact intersection of trajectories is more difficult to attain than in the two dimensional case, because the profiles of two adjacent column sections may miss each other in additional dimensions.<sup>36</sup> A feasible side rectifier design for a

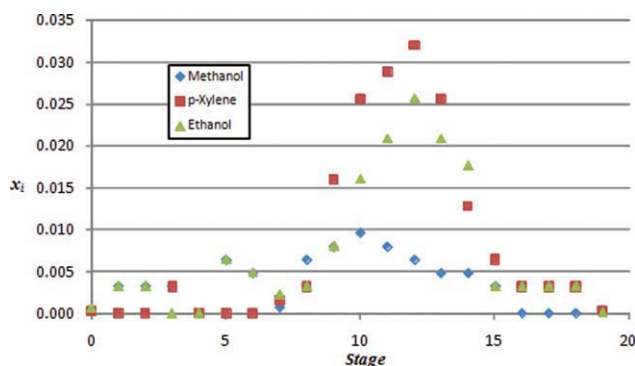


**Figure 18.** A plot of the absolute difference between compositions predicted by AspenPlus and temperature collocation on each stage.

[Color figure can be viewed in the online issue, which is available at [wileyonlinelibrary.com](http://wileyonlinelibrary.com).]

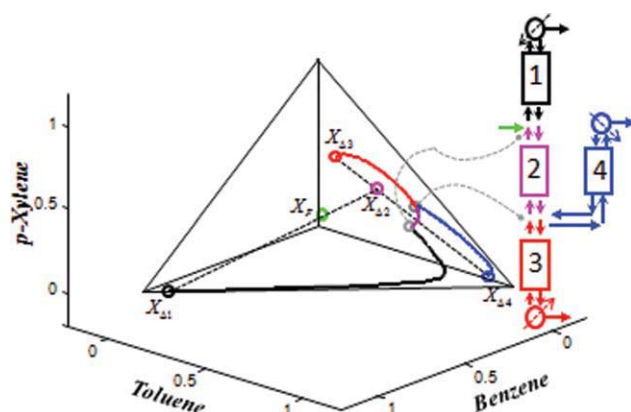


**Figure 19. A feasible side rectifier design for the benzene/toluene/p-xylene/phenol system, showing areas of profile intersection and the location of all respective difference points.**

[Color figure can be viewed in the online issue, which is available at [www.interscience.wiley.com](http://www.interscience.wiley.com).]

nonideal quaternary mixture of benzene/toluene/p-xylene/phenol is shown in Figure 19 along with all relevant parameters summarized in Table 3.

Intuitively for a higher order single side rectifying or stripping unit, at least one product stream will not contain a high purity of a single component (bottoms product in this case), but once these product specifications have been selected, the design procedure remains the same. Notice that the linear relationship between the relevant difference points still holds and that the profile intersection criterion is the same as for the ternary case.

Although the extension to higher order mixtures is, in principle, a mere extrapolation of the procedures presented here it does involve more careful selection of variables. An additional component in a single side stripper/rectifier arrangement requires that two external degrees of freedom be set and may thus require some additional design experience. Because the composition profiles are extremely dependant on the  $X_{\Delta}$  choices of the designer, more components introduce additional difficulties with respect to finding profile intersections. This has been shown in a recent paper where a 10 component separation synthesis problem was successfully dealt with in a simple column using the BPD as a feasibility criterion.<sup>37</sup> This design was performed for a variety of feeds and product specifications and was subsequently validated with Aspen Plus. Although the graphical characteristics of the method are somewhat lost in higher order systems, the algebraic BPD criterion naturally extends to these systems. It should be noted that for single side rectifying/stripping unit there are, however, only two internal

degrees of freedom regardless of the number of components. Thus, the feasibility diagrams shown in Figure 11 will always be applicable. If, however, there are multiple thermal couplings with multiple stream splits this diagram also becomes multidimensional.

Furthermore, it has been well publicized that composition profiles that originate near pure component vertices are extremely sensitive to the presence of trace components,<sup>38</sup> and therefore, the refluxes and stage numbers (and feasibility) may differ vastly for only small changes in composition. However, the advantage of using the minimum BPD approach in dealing with both these inherent difficulties (high-order systems and trace compounds) is that a small BPD function value indicates closeness to a feasible design, and can aid in steering the designer toward a feasible design, rather than being merely a Boolean success or fail intersection criterion. Thus, by tracking the BPD function value the designer knows how far away a feasible design may be and may adjust parameters accordingly.

## Discussion and Conclusions

In this work, a systematical procedure has been proposed to rigorously design and analyze thermally coupled sidestream units, without making use of simplifying assumptions such as constant relative volatilities, sharp splits, or pinched column profiles. The method combines the advantages of the column profile map technique to assess parameter interaction of a specific configuration, with the temperature collocation technique to rigorously search for liquid composition profile intersections. This methodology allows a unique graphical insight into the challenging problem of thermally coupled columns. The interaction of internal process variables can easily be assessed with this method and furthermore methods are presented to identify superior design decisions and immediately eliminate poor design choices, based on reboiler duty, column height, and thermodynamic efficiency. Although the aim of the article is not to search for optimal design solutions, it has been shown that using these novel design techniques, the designer can make informed design decisions to assess feasibility relatively quickly. Furthermore, the inverse design procedure is presented, which allows one to find key operating parameters such as the feed tray and side-draw tray, by setting product specifications and searching feasibility. Designs can be validated with an industrially accepted process simulator such as AspenPlus and in our examples typically lead to fast convergence without further adjustment. Future work in this area includes applying this technique to fully thermally coupled columns such as the Petlyuk and Kaibel columns as well as searching for improvements and a better understanding on other applications of thermally coupled sidestream columns, such as crude distillation. The methods proposed here

**Table 3. Stream Table for a Benzene/Toluene/p-Xylene/Phenol System**

Column Section	Difference Point	Reflux	Net Flow ( $\Delta$ ) (mol/s)
Feed	[0.250; 0.250; 0.250; 0.250]	—	1 (pure liquid)
CS <sub>1</sub>	[0.929; 0.071; 2.38 E -4; 2.20 E -5]	4.743	0.260
CS <sub>2</sub>	[0.011; 0.313; 0.338; 0.339]	-3.015	0.740
CS <sub>3</sub>	[2.61 E -5; 0.092; 0.447; 0.461]	-4.830	-0.540
CS <sub>4</sub>	[0.042; 0.910; 0.042; 0.006]	1.900	0.200

are also ideal for the design of bio-refineries and azeotropic distillation problems.

## Acknowledgments

Financial support by DOE Grant: DE-FG36-06GO16104 is gratefully acknowledged. We thank Dr. Chau-Chyan Chen from AspenTech for providing an Aspen research license and Dr. Gerardo Ruiz for his valuable discussions. They also thank David Glasser and Diane Hildebrandt from the University of the Witwatersrand for facilitating the exchange.

## Literature Cited

1. U.S. Department of Energy (DOE). Technical Topic Description. 2005. Available at: [www.doe.gov](http://www.doe.gov). Accessed on 30 October 2010.
2. Wolff EA, Skogestad S. Operation of integrated three-product (Petlyuk) distillation columns. *Ind Eng Chem Res.* 1995;34:2094–2103.
3. Agrawal R, Fidkowski ZT. Are thermally coupled distillation columns always thermodynamically more efficient for ternary distillations? *Ind Eng Chem Res.* 1998;37:3444–3454.
4. Fidkowski ZT, Agrawal R. Multicomponent thermally coupled systems of distillation columns at minimum reflux. *AIChE J.* 2001;47:2713–2724.
5. Brüggemann S, Marquardt W. Rapid screening of design alternatives for nonideal multiproduct distillation processes. *Comput Chem Eng.* 2004;29:165–179.
6. Engelen HK, Skogestad S. Multi-effect distillation applied to an industrial case study. *Chem Eng Process.* 2005;44:819–826.
7. Watkins RN. *Petroleum Refinery Distillation*. Houston: Gulf Publishing Co., 1979.
8. Petlyuk FB. *Distillation Theory and Its Application to Optimal Design of Separation Unit*. Cambridge: Cambridge University Press, 2004.
9. Emmrich G, Gehrke H, Ranke U. The progressive extractive distillation arrangement for the morphylane extractive distillation process. *Chem Ing Tech.* 2001;73:715.
10. Frey RM, Doherty MF, Douglas JM, Malone MF. Controlling thermally linked distillation columns. *Ind Eng Chem Process Des Dev.* 1984;23:483–490.
11. Alstad V, Halvorsen IJ, Skogestad S. Optimal operation of a petlyuk distillation column: energy savings by over-fractionating. *Computer Aided Chemical Engineering*. Elsevier, 2004;18:547–552.
12. Alberto Porras-Rodríguez J, Hernández-Escoto H, Gabriel Segovia-Hernández J, Hernández S. Design and control of thermally coupled and heat integrated distillation sequences for quaternary separations. *Computer Aided Chemical Engineering*. Elsevier, 2007;24:889–894.
13. Halvorsen IJ, Skogestad S. Optimizing control of Petlyuk distillation: understanding the steady-state behavior. *Comput Chem Eng.* 1997;21(Suppl 1):S249–S254.
14. Hernandez S, Jimenez A. Controllability analysis of thermally coupled distillation systems. *Ind Eng Chem Res.* 1999;38:3957–3963.
15. Segovia-Hernández JG, Hernández S, Jiménez A. Analysis of dynamic properties of alternative sequences to the Petlyuk column. *Comput Chem Eng.* 2005;29:1389–1399.
16. Kaibel G, Schoenmakers H. Process synthesis and design in industrial practice. *Computer Aided Chemical Engineering*. Elsevier, 2002;10:9–22.
17. Glinos KN, Malone MF. Design of sidestream distillation columns. *Ind Eng Chem Process Des Dev.* 1985;24:822–828.
18. Glinos K, Malone MF. Minimum vapor flows in a distillation column with a sidestream stripper. *Ind Eng Chem Res Process Des.* 1985;24:1087–1090.
19. Fidkowski Z, Krolikowski LW. Minimum energy requirements of thermally coupled distillation systems. *AIChE J.* 1987;33:643–653.
20. Lucia A, Amale A, Taylor R. Energy efficient hybrid separation processes. *Ind Eng Chem Res.* 2006;45:8319–8328.
21. Lucia A, McCallum BR. Energy targeting and minimum energy distillation column sequences. *Comput Chem Eng.* 2010;34:931–942.
22. Lucia A, McCallum BR. Energy targeting and minimum energy distillation column sequences. *Comput Chem Eng.* 2010;34:931–942.
23. Tapp M, Holland ST, Hildebrandt D, Glasser D. Column Profile maps. 1. Derivation and interpretation. *Ind Eng Chem Res.* 2004;43:364–374.
24. Holland ST, Tapp M, Hildebrandt D, Glasser D, Hausberger B. Novel separation system design using “moving triangles.” *Comput Chem Eng.* 2004;29:181–189.
25. Holland ST, Abbas R, Hildebrandt D, Glasser D. Complex column design by application of column profile map techniques: sharp-split Petlyuk column design. *Ind Eng Chem Res.* 2010;49:327–349.
26. Zhang L, Linninger AA. Temperature collocation algorithm for fast and robust distillation design. *Ind Eng Chem Res.* 2004;43:3163–3182.
27. Ruiz GJ, Kim S, Moon J, Zhang L, Linninger AA. *Design and optimization of energy efficient complex separation networks*. In: Linninger AA, El-Halwagi M, editors. *7th International Conference on Foundations of Computer-Aided Process Design*. Boca Raton, FL: CRC Press, 2009:747–755.
28. Van Dongen DB, Doherty MF. Design and synthesis of homogeneous azeotropic distillations. 1. Problem formulation for a single column. *Ind Eng Chem Fundam.* 1985;24:454–463.
29. Holland ST, Tapp M, Hildebrandt D, Glasser D. Column profile maps. 2. Singular points and phase diagram behaviour in ideal and nonideal systems. *Ind Eng Chem Res.* 2004;43:3590–3603.
30. Zhang L, Linninger AA. Towards computer-aided separation synthesis. *AIChE J.* 2006;52:1392–1409.
31. Agrawal R. Synthesis of distillation column configurations for a multicomponent separation. *Ind Eng Chem Res.* 1996;35:1059–1071.
32. Sargent RWH, Gaminibandara K. Optimal Design of Plate Distillation Columns. In: Dixon, L. C. W., editor. *Optimization in Action*; New York: Academic Press, 1976.
33. Freshwater DC, Henry BD. The optimal configuration of multicomponent distillation trains. *Chem Eng.* 1975;301:533–536.
34. Seader JD, Henley EJ. *Separation Process Principles*. Hoboken, NJ: Wiley, 2006.
35. Kister HZ. *Distillation Design*. New York: McGraw-Hill, 1992.
36. Julka V, Doherty MF. Geometric behavior and minimum flows for nonideal multicomponent distillation. *Chem Eng Sci.* 1990;45:1801–1822.
37. Kim SB, Ruiz GJ, Linninger AA. Rigorous separation design. 1. Multicomponent mixtures, nonideal mixtures, and prefractionating column networks. *Ind Eng Chem Res.* 2010;49:6499–6513.
38. Levy SG, Van Dongen DB, Doherty MF. Design and synthesis of homogeneous azeotropic distillations. 2. Minimum reflux calculations for nonideal and azeotropic columns. *Ind Eng Chem Fundam.* 1985;24:463–474.

Manuscript received July 19, 2010, and revision received Sept. 15, 2010.